

Intrinsic Redshifts in Normal Spiral Galaxies

David G. Russell

Owego Free Academy, Owego, NY 13827 USA

Russeld1@oagw.stier.org

Abstract

The Tully-Fisher (TF) relation calibrated in both the B-band and the I-band indicates that (1) the redshift distribution of Virgo Cluster spirals has a morphological dependence that is inconsistent with a peculiar velocity interpretation. (2) Galaxies of morphology similar to ScI galaxies have a systematic excess redshift component relative to the redshift expected from a Hubble Constant of $72 \text{ km s}^{-1} \text{ Mpc}^{-1}$. (3) Pairs and groups of galaxies exist for which the TF relation provides excellent agreement among individual members, but for which the group redshift deviates strongly from the predictions of the Hubble Relation. It is again found that morphology plays a role as these galaxies are all of Hubble types Sbc and Sc. The overall results of this study indicate that normal Sbc and Sc galaxies have a systematic excess redshift component relative to the predictions of the standard Hubble relation assuming a Hubble Constant of $72 \text{ km s}^{-1} \text{ Mpc}^{-1}$. The excess redshifts identified in this analysis are consistent with the expectations of previous claims for non-cosmological (intrinsic) redshifts.

1. Introduction

Strong empirical evidence has accumulated that many quasars are not at large cosmological distances as is expected from the traditional redshift-distance relation (Arp 1986; Arp 1998a; Chu et al 1998; Arp 1999; Bell 2002; Lopez-Coredaira&Gutierrez 2002). The emerging picture is that quasars can be ejected from active Seyfert galaxies as high redshift objects that evolve to lower redshifts as they age (Arp 1998b, Bell 2002). Recently, Lopez-Corredoira&Gutierrez (2002) demonstrated that a pair of high z objects are present in a luminous filament apparently connecting the Seyfert galaxy NGC 7603 to the companion galaxy NGC 7603B which is previously know to have a discordant redshift. It was noted by Arp (1980) that the NGC 7603/NGC 7603B pair is one example of a class of objects in which a lower redshift galaxy appears to be physically connected by a luminous bridge to a companion with a discordant high redshift. Associations between high and low redshift companions are generally dismissed as accidental alignments. As stated by Arp (1980) “But in the end, no matter how convincing the connection is, it would be possible to take the position that it is an accident.”

The most thorough investigations into the existence of non-velocity redshifts in normal galaxies have been presented by Arp (1987, 1988, 1990,1994,1998a,b) and Russell (2002). Arp demonstrated that Sbc/Sc type galaxies have excess redshifts relative to Sb galaxies in the Virgo cluster (1988) and in the general field (1990). Russell (2002) utilized linear diameters as a further test of this discrepancy and confirmed this behavior.

The Hubble Key Project (Freedman et al 2001) has provided an increased number of calibrators for the Tully-Fisher relation. Russell (2002) demonstrated that scatter in the Tully-Fisher relation can be reduced when morphological type dependence is properly accounted for in calibrating the Tully-Fisher relationship. Using type dependent Tully-Fisher relations in both the B and the I-bands it is shown that ScI galaxies and a number of small groups of galaxies possess sizeable systematic excess redshifts which suggest the existence of an intrinsic redshift component.

2. Type dependent Tully-Fisher relations

2.1 Calibration of type dependent Tully-Fisher relations

Russell (2002 – R02) demonstrated that the Tully-Fisher relation is subject to morphological and luminosity class type dependence such that galaxies of morphology similar to ScI galaxies and Seyfert galaxies are more luminous at a given rotational velocity than Sab/Sb galaxies and Sc galaxies of luminosity classes II-III to IV (figure 1). In this analysis, two morphological groups are identified for calibration of the Tully-Fisher relation. The ScI group includes SbcI, SbcI-II, ScI, ScI-II, and Seyfert galaxies (filled circles in figure 1). The Sb/ScIII group includes all Sab/Sb/Sbc/Sc galaxies that are not in the ScI group. For this analysis, the type dependent equations have been calibrated using corrected B-band and I-band magnitudes from the LEDA database following the calibration procedures described in R02. The Tully-Fisher (TF) calibrator data is provided in Table I and Table II gives the B-band and I-band zero points. Figure 1 is a plot of the TF relation in the B-band and the B-band and I-band TF relations are:

B-band:

$$\mu = 19.85(\pm 0.16) + 5.24(\pm 0.10)(\log V_{\max} - 2.2) + B_{tc} \quad \text{Sb/ScIII group}$$

$$\mu = 20.44(\pm 0.09) + 4.91(\pm 0.20)(\log V_{\max} - 2.2) + B_{tc} \quad \text{ScI group}$$

I-band:

$$\mu = 21.29(\pm 0.24) + 7.12(\pm 0.19)(\log V_{\max} - 2.2) + I_{tc} \quad \text{Sb/ScIII group}$$

$$\mu = 21.55(\pm 0.07) + 7.22(\pm 0.10)(\log V_{\max} - 2.2) + I_{tc} \quad \text{ScI group}$$

The major concern with the procedure adopted here for calibration of the TF relation is the smaller number of calibrators available for slope and zero point determination when the calibrators are split into type dependent samples. However, a few points lessen this concern. First, the slopes of the Sb/ScIII and ScI type dependent relations are very close in both the B-band and the I-band. If the complete calibrator samples were used for determining the slope, then the slopes would be 5.75 for the B-band relation and 7.39 for the I-band relation. Second, the overall scatter is smaller with the use of the type dependent equations. In the B-band the 1σ scatter relative to the calibrator

distance moduli is 0.09 mag for the ScI group and 0.16 mag for the Sb/ScIII group. In the I-band the 1σ scatter is 0.07 mag and 0.24 mag respectively. With a single calibration the Hubble Key Project (Sakai et al 2000) found TF scatter of 0.45 mag (B-band) and 0.37 mag (I-band) for a sample of 21 cepheid calibrators. Finally, it is noted that Tully&Pierce (2000) found that the slope and zero point derived from their cluster template relations were virtually identical to the slope and zero point derived from the calibrator sample alone. This suggests that useful TF relations can be derived from the calibrator samples.

If the type effect is not accounted for, ScI group galaxies will have systematically underestimated TF distances while Sb/ScIII group galaxies will have systematically overestimated TF distances. This effect is illustrated with a sample drawn from the Ursa Major cluster sample of Verheijen (2001) which are listed in Table III. Rotational velocities utilized for calculating TF distances for this sample are V_{flat} from Verheijen (2001). With the use of Type dependent equations, the mean distance modulus of the ScI group galaxies agrees within 0.04 mag of the mean distance modulus to the cluster. However, when a single calibration is utilized the mean distance modulus of the ScI group is less than the mean distance modulus of the Sb/ScIII group sample by 0.45 mag (B-band) and 0.27 mag (I-band).

2.2 The Tully-Fisher Sample

For this analysis we have selected (1) Galaxies within the Virgo cluster with TF data in the LEDA database. (2) Galaxies of ScI group morphology (SbcI, SbcI-II, ScI, ScI-II) and rotational velocities derived from optical rotation curves in Mathewson&Ford (1996) or rotational velocities derived from hydrogen linewidths in Giovanelli et al (1997). (3) Small groups and pairs of galaxies with rotational velocities in Mathewson/Ford. ScI group galaxies selected were restricted to those with inclinations between 30 and 80 degrees and with absorption corrections in LEDA ($a_g + a_i$) less than 1.00 mag. Galaxies in the ScI group were also restricted to those with mean surface brightness in the D_{25} isophote (bri_{25} in LEDA) from 22.35 to 23.99 – which covers the surface brightness range of the calibrators. To reduce the effect of inclination errors upon corrected magnitudes, galaxies were eliminated for which the LEDA inclination has a difference from the Mathewson/Ford or Giovanelli et al inclination that exceeds 7 degrees. After these restrictions, the sample size for the ScI group was 83 galaxies.

3. Evidence for non-cosmological redshifts

3.1 The Virgo Cluster

The Virgo cluster is the nearest major cluster for which evidence for intrinsic redshifts in normal galaxies has previously been indicated (Arp 1988). Extensive data for TF analysis is available in the LEDA database and the recent surface brightness fluctuation study of E/SO galaxies of Tonry et al (2001) provides additional distances. In Table IV, the mean distances and redshift velocities of subsamples of Virgo cluster galaxies are provided. While all subsamples have mean distances within 1.4 Mpc of the mean distance for the full sample of 77 galaxies, two outstanding anomalies emerge in Table IV. First, there are dramatic differences in mean redshift that are dependent upon morphological type. Second, galaxies with linear diameters less than 20 kpc within the E/SO group and galaxies with rotational velocities less than $\log v = 2.200$ within the SO-a to Sbc group have significantly larger mean redshifts than the giant galaxies within the same morphological groups.

The most dramatic result in Table IV is the extreme excess redshifts of the ScI/Seyfert group. Since three of these galaxies (NGC 4321, NGC 4535, NGC 4536) have Cepheid distances it is unlikely that this phenomenon results from inaccurate distances (see also Arp 2002). The result cannot be attributed to the morphological density relation (Dressler 1980) because the redshift excess is systematically positive and the galaxies in question are on both the front and backside of the mean cluster distance.

The unusual redshift-morphology result is further illustrated in Table V for which the distances, redshifts and peculiar motions (calculated with V_{vir} in LEDA assuming $H_0 = 72 \text{ km s}^{-1} \text{ Mpc}^{-1}$) are given for all galaxies within the core distance of 13-20 Mpc and with linear diameters exceeding 20 kpc. Note that the giant Sab/Sb galaxies have apparent large negative peculiar motions in contrast to the large positive apparent peculiar motions of the ScI/Seyfert group. *Adopting a strict velocity interpretation of galaxy redshifts requires that as a group the giant Sb galaxies are approaching the Milky Way with a mean velocity of -898 km s^{-1} while the giant ScI galaxies are receding from the Milky Way with a mean velocity of $+824 \text{ km s}^{-1}$.*

The second discrepant result in Table IV is the excess redshift that galaxies smaller than 20 kpc have relative to the giant galaxies in the E/SO and Sb groups. As with morphologically selected subsamples, the diameter selected subsamples are close to the mean cluster distance. However, relative to the larger galaxies in each group, the small galaxies have a systematic excess redshift of 417 km s^{-1} for the elliptical group and 277 km s^{-1} for the Sb group. This excess extends to the dwarf

elliptical and spheroidal galaxies in Virgo (Binggeli, Popescu, & Tammann 1993). Similar excesses for smaller companions have also been demonstrated for the Local Group and M-81 group (Arp 1988, 1994).

The morphological dichotomy of redshifts in the large spirals of Virgo is incompatible with a peculiar velocity interpretation. If peculiar motions were responsible for deviations from the velocities predicted by the Hubble relation, then as many negative as positive peculiar motions should be expected in both groups. Instead the trend is clearly systematic with Sb galaxies systematically deficient in redshift and ScI galaxies systematically excessive in redshift. But this is exactly what is seen in the Local Group and M-81 group for which the largest Sb type spirals have the smallest redshifts (Arp 1994).

An alternative explanation is that the excess redshifts of the ScI group are non-velocity or intrinsic. A model that may account for both the excess redshift of the ScI group and the redshift deficit of the Sb group will be noted in section 4.

3.2. ScI galaxies

Table VI lists the 83 ScI group galaxies utilized in this analysis. In figures 2 and 3 the Hubble relation for these galaxies is plotted for the B-band and I-band TF relations respectively. The solid line in figures 2 and 3 represents a Hubble Constant of $72 \text{ km s}^{-1} \text{ Mpc}^{-1}$ (Freedman et al 2001). It is clearly seen that the ScI galaxies have a systematic excess redshift relative to a Hubble Constant of $72 \text{ km s}^{-1} \text{ Mpc}^{-1}$. Since the result is the same for both the B-band and the I-band TF relations it is unlikely that magnitude errors are the source of the problem. It is also important to note that the use of type dependent TF equations is not the reason for the difference between redshift and TF distances either. The ScI group TF zero point is 0.59 mag larger than the Sb/ScIII group zero point in the B-band and 0.26 mag larger in the I-band. *If a single TF calibration for all types was utilized, the TF distance moduli of the ScI group galaxies would be reduced and thus would make the discrepancy even more extreme.*

The bulk of the sample has rotational velocities derived from optical rotation curves by Mathewson & Ford (1996 - MF). Since the MF rotation curves were demonstrated to have an internal consistency of 10 km s^{-1} or better it is unlikely that rotational velocity errors are the source of the deviation from the predicted Hubble relation. It should also be noted that if rotational velocity errors are the explanation, then the MF optical rotation curves systematically underestimate the true

rotational velocity. However, Verheijen (2001) has noted that the velocity at which the rotation curve becomes flat may be a better estimate of the true rotational velocity than the maximum rotational velocity of a rotation curve. So it would not be unexpected that many of the ScI galaxies in our sample have overestimated rotational velocities and TF distances too large. Correcting for these errors would make the mean deviation from the predicted Hubble relation even more extreme.

If it is assumed that there are no intrinsic redshifts, then the ScI group sample utilized here indicates a Hubble constant of $86 \text{ km s}^{-1} \text{ Mpc}^{-1}$ (B-band) or $85 \text{ km s}^{-1} \text{ Mpc}^{-1}$ (I-band). The systematic excess redshift of ScI galaxies was previously demonstrated by Arp (1990) with the B-band TF relation for a large sample of ScI type galaxies. The results of this study reinforce and improve upon the earlier result of Arp in several ways: (1) Both B and I-band TF relations have been utilized and the TF relation is calibrated from a larger number of Cepheid calibrators. The 1σ scatter of the relation is less than 0.10 mag for both the B-band and I-band among the calibrators and no ScI group calibrator has a TF distance modulus that differs from the Cepheid distance modulus by more than 0.15 mag. (B-band) or 0.24 mag. (I-band). (2) Optical rotation curve rotational velocities were utilized in this study while Arp (1990) utilized hydrogen linewidths and thus both methods of measuring rotational velocity produce the same result. (3) The sample utilized here is drawn independently of Arp's sample and extends to larger distances and higher redshifts.

In a number of cases the individual discrepancy between the TF distance and the $H_0=72$ redshift distance is significantly larger than can be accounted for by TF errors and therefore strongly supports the existence of intrinsic redshifts. For example, the galaxy ESO 147-5 has a TF distance modulus of 34.65 (B-band) or 34.56 (I-band) while the redshift distance modulus is 35.86 – a discrepancy of 1.21 to 1.30 mag. ESO 147-5 thus has an excess redshift of $+4551 \text{ km s}^{-1}$. An excess redshift this large cannot be a peculiar motion or result from a large scale flow and therefore indicates the existence of a non-cosmological (intrinsic) redshift component. In the next section it is shown that this interpretation is supported by a number of pairs and small groups of galaxies.

3.3 Pairs and Groups with intrinsic redshifts

Table VII lists TF distance moduli for eight pairs/groups of galaxies with rotational velocities in Mathewson & Ford (1996). Several important points must be made regarding these groups. (1) Four of the groups include ScI galaxies with extreme excess redshifts that were discussed in the previous section. (2) The scatter in TF distance moduli among the galaxies in these pairs/groups is

consistent with the small TF scatter of the calibrators. (3) The galaxies in these groups are all (except the edge-on galaxy ESO 243-8) types Sbc or Sc as classified in LEDA. (4) The groups exhibit extreme excess redshifts comparable with the most extreme examples among the ScI group galaxies as is demonstrated in Table VIII.

The close agreement of the TF distance moduli for the galaxies in these eight pairs/groups makes it unlikely that the TF distances suffer from significant errors and therefore these groups verify the existence of intrinsic redshifts indicated by the ScI group galaxies. The Hubble relation for these pairs and groups is plotted in figure 4. It can be seen that the mean redshifts of these groups deviate from the predicted Hubble relation by 1021 km s^{-1} to 4746 km s^{-1} . For example, the ESO 549-30 group includes 6 galaxies with a mean TF distance modulus of 34.22. The redshift distance modulus indicated by the group mean velocity is 35.27 and requires that either all 6 galaxies have TF distance modulus errors of $\sim 1.00 \text{ mag}$ or that the galaxies in the group have a mean intrinsic redshift of $+3140 \text{ km s}^{-1}$.

4. Discussion and Conclusion

The results of this analysis support the previous conclusions of Arp (1988, 1990, 1998a) that many late type spiral galaxies contain an excess redshift component that may reasonably be interpreted as non-cosmological or intrinsic. It was also found that the giant Sab/Sb galaxies in Virgo have extreme negative peculiar motions or intrinsic redshifts. Arp (1988 – and references therein) noted that the redshift deficit of Sb galaxies relative to other morphological types in clusters may be a common phenomenon. A distant cluster of galaxies in Serpens with TF data in the LEDA database was identified which also demonstrates this behavior. The individual galaxies are listed in Table IX and the group is plotted in figure 5. It can be seen in figure 5 that the galaxies in this group form a filament with the Sa galaxy PGC 55828 located near the center of the filament (indicated by the filled triangle in figure 5). The mean distance of the group is 154.2 Mpc and the mean redshift is 10835 km s^{-1} . Thus this group indicates a Hubble Constant of $70.3 \text{ km s}^{-1} \text{ Mpc}^{-1}$ which is consistent with the results of Freedman et al (2001). However, the redshift-morphology behavior of the Virgo cluster is repeated in this distant group as shown in Table X. The mean distance of the Sa/Sb and Sbc/Sc subsamples are in excellent agreement, but the mean redshift of the Sbc/Sc galaxies is 1507 km s^{-1} greater than the Sa/Sb galaxies. This difference would increase to 1748 km s^{-1} if the single Sb group galaxy with $\log v_{\text{rad}} < 2.200$ is eliminated from the Sb group sample. In addition, individual galaxies exist within the Serpens filament that have extreme deviations from the

mean cluster redshift. The SBbc galaxy PGC 55724 has a redshift of 15065 which is 4230 km s^{-1} greater than the cluster mean. In contrast, the central Sa galaxy PGC 55828 has a redshift of 6989 km s^{-1} which is 3846 km s^{-1} less than the cluster mean. In the traditional interpretation of galaxy redshifts PGC 55828 is a foreground galaxy. But in that view it would have to be accepted that PGC 55828 has an incorrect TF distance modulus that by chance matches the TF distance moduli of 16 other galaxies forming a real group. At the same time it would have to be accepted that PGC 55724 and PGC 56169 are a pair of background galaxies which have incorrect TF distance moduli that also by chance match the TF distance moduli of 16 other galaxies in a real group. It is also important to note that both PGC 55828 and PGC 55724 exhibit normal double-horned hydrogen profiles in Freudling, Haynes, & Giovanelli (1992) – which reinforces that large TF errors are unlikely to be the reason for the difference between the redshift and TF distance moduli.

Narlikar&Arp (1993) provided a model which may explain the intrinsic redshift behavior identified in this analysis. In the model of Narlikar&Arp (1993) galaxy redshifts are a function of age such that younger galaxies have larger redshifts than older galaxies at the same distance. The results of this analysis suggest that late type Sbc/Sc galaxies tend to have larger redshifts than early type Sa/Sb galaxies. In the Narlikar&Arp model this would indicate that late type spirals are generally younger than early type spirals. For PGC 55828, the low redshift leads to the interpretation that it is the oldest galaxy in the filament according to the Narlikar&Arp model.

Regardless of the theoretical explanation for intrinsic redshifts, the empirical results of this study strongly indicate that intrinsic redshifts exist in normal galaxies. Tully-Fisher distances in both the B-band and the I-band have been used to establish that ScI group galaxies have a systematic excess redshift relative to redshifts predicted with a Hubble Constant of $72 \text{ km s}^{-1} \text{ Mpc}^{-1}$. These excess redshifts must be even more extreme if proponents of a lower Hubble Constant are correct (eg. Ekholm et al 1999; Parodi et al 2000; Sandage 2002). In the most extreme cases the difference between redshift and Tully-Fisher distances implies redshift excesses larger than 3000 km s^{-1} for groups and up to $+4550 \text{ km s}^{-1}$ for individual galaxies.

Acknowledgements:

This research has made use of the Lyon-Meudon extragalactic Database (LEDA) compiled by the LEDA team at the CRAL-Observatoire de Lyon (France).

References:

- Arp, H. 1980, *Astrophys. J.* 239, 469
- Arp, H. 1987. *Quasars, Redshifts, and Controversy* (Berkeley: Interstellar Media)
- Arp, H. 1988, *Astron. Astrophys.* 202, 70
- Arp, H. 1990, *Astrophys. Space Sci.* 167, 183
- Arp, H. 1994, *Astrophys. J.* 430, 74
- Arp, H. 1998a, *Seeing Red* (Montreal: Apeiron)
- Arp, H. 1998b, *Astrophys. J.* 496, 661
- Arp, H. 1999, *Astron. Astrophys.* 341, L5-L8
- Arp, H. 2002, *Astrophys. J.* 571, 615
- Bell, M.B. 2002, *Astrophys. J.* 566, 705
- Binggeli, B., Popescu, C.C., & Tammann, G. 1003, *Astron. Astrophys. Suppl.* 98, 275
- Chu, Y. et al 1998, *Astrophys. J.* 500, 596
- Dressler, A. 1980, *Astrophys. J.* 236, 351
- Drozdovsky, I. & Karachentsev, I. 2000, *Astron. Astrophys. Suppl.* 142, 425
- Ekhholm, T., Teerikorpi, P., Theureau, G., Hanski, M., Paturel, G., Bottinelli, L., & Gouguenheim, L. 1999, *Astron. Astrophys.* 347, 99
- Freedman, W., Madore, B., Gibson, B., Ferrarese, L., Kelson, P., et al 2001, *Astrophys. J.* 553, 47
- Freudling, W., Haynes, M., Giovanelli, R. 1992, *Astrophys. J. Suppl.* 79, 157
- Giovanelli, R. et al 1997, *Astron. J.* 113, 22
- Lopez-Corredoira, M. & Gutierrez, C. 2002, *Astron. Astrophys.* 390, L15-L18
- Macri, L. et al 2001, *Astrophys. J.* 559, 243
- Mathewson, D. & Ford, V. 1996, *Astrophys. J. Suppl.* 107,97 (MF)
- Narlikar, J. & Arp, H. 1993, *Astrophys. J.* 405, 51
- Newman, J., Zepf, S., Davis, M., Freedman, W., Madore, B. et al 1999, *Astrophys. J.* 523, 506
- Parodi, B., Saha, A., Sandage, A., Tammann, G. 2000, *Astrophys. J.* 540, 634
- Russell, D. 2002, *Astrophys. J.* 565, 681
- Saha, A. et al 2001, *Astrophys. J.* 551, 973
- Sakai, S. et al 2000, *Astrophys. J.* 529, 698
- Sandage, A. 2002, *Astron. J.* 123, 1179
- Tonry, J.L. et al 2001, *Astrophys. J.* 546, 681

Tully, R. & Pierce, M. 2000, *Astrophys. J.* 533, 744

Verheijen, M. 2001, *Astrophys. J.* 563, 694

Table I: Tully-Fisher Calibrator Data

1	2	3	4	5	6	7	8
Galaxy	Type	btc	Itc	incl	logVrot	m-Mcalib	Ref.
Sb/ScIII group							
N224	SbI-II	3.20	1.47	78	2.411	24.48	1
N2841	SbI	9.51	7.91	67	2.488	30.74	2
N3031	SabI-II	7.12	5.41	59	2.375	27.80	1
N3351	SBbII	10.06	8.32	48	2.232	30.00	1
N3368	SBabII	9.75	7.99	49	2.336	30.11	1
N4527	SBbcII	10.62	8.91	74	2.260	30.75	3
N4548	SBbI-II	10.66	8.89	38	2.279	31.05	1
N4639	SBbcII-III	11.81	10.27	54	2.215	31.71	1
N4725	SBabI.3	9.75	8.04	64	2.325	30.46	1
N598	ScII-III	5.73		55	2.011	24.62	1
N2090	ScII-III	10.94	9.35	69	2.146	30.35	1
N2403	SBcIII	8.24	7.32	59	2.104	27.54	1
N2541	SBcIII-IV	11.61	10.53	63	1.989	30.25	1
N3319	SBcII	11.33	10.39	57	2.043	30.62	1
N4414	ScII-III	10.65	8.87	57	2.344	31.24	1
ScI group							
N1365	SBbI(sy)	9.90	8.18	47	2.397	31.27	1
N1425	SbII.2	10.83	9.55	65	2.270	31.70	1
N2903	SBbcI-II	8.86	7.58	64	2.282	29.75	4
N3198	SBcII	10.22	9.22	68	2.184	30.70	1
N3627	SBbII(sy)	8.98	7.54	54	2.326	30.01	1
N4258	SBbcII-III(sy)	8.38	7.04	72	2.327	29.51	1
N4321	ScI	9.79	8.39	30	2.338	30.91	1
N4535	SBcI-II	10.35	8.89	43	2.270	30.99	1
N4536	SBbcI-II	10.43	9.15	68	2.230	30.87	1
N4603	SBcI.3	11.35	9.86	49	2.358	32.61	5
N5457	ScdI	8.24	6.99	21	2.315	29.13	1
N7331	SbcI-II	9.25	7.70	67	2.424	30.84	1

References:

1 - Freedman et al 2001; 2 – Macri et al 2001; 3 - Saha et al 2001; 4 - Drozdovsky&Karchentsev 2000; 5 – Newman et al 1999

Table II: Calibration of the B-band and I-band Tully-Fisher Relations

	1	2	3	4	5	6	7
Galaxy	zero pt B	m-M TF _B	m-Merr B	zero pt I	m-M TF _I	m-Merr I	
Sb/ScIII group							
N224	20.17	24.16	-0.32	21.51	24.26	-0.22	
N2841	19.72	30.87	0.13	20.78	31.25	0.51	
N3031	19.76	27.71	-0.09	21.14	27.95	0.15	
N3351	19.77	30.08	0.08	21.45	29.84	-0.16	
N3368	19.65	30.31	0.20	21.15	30.25	0.14	
N4527	19.82	30.78	0.03	21.41	30.63	-0.12	
N4548	19.98	30.92	-0.13	21.60	30.74	-0.31	
N4639	19.82	31.74	0.03	21.33	31.67	-0.04	
N4725	20.06	30.26	-0.20	21.53	30.22	-0.24	
N598	19.88	24.59	-0.03				
N2090	19.69	30.51	0.16	21.38	30.26	-0.09	
N2403	19.80	27.59	0.05	20.90	27.93	0.39	
N2541	19.75	30.35	0.10	21.22	30.32	0.07	
N3319	20.11	30.36	-0.26	21.35	30.56	-0.06	
N4414	19.84	31.25	0.01	21.34	31.25	-0.05	
			$\sigma=0.16$				$\sigma=0.24$
ScI group							
N1365	20.40	31.31	0.04	21.67	31.15	-0.12	
N1425	20.53	31.61	-0.09	21.64	31.61	-0.09	
N2903	20.49	29.70	-0.05	21.58	29.72	-0.03	
N3198	20.56	30.58	-0.12	21.60	30.65	-0.05	
N3627	20.41	30.04	0.03	21.56	30.00	-0.01	
N4258	20.51	29.44	-0.07	21.55	29.51	0.00	
N4321	20.44	30.91	0.00	21.52	30.94	0.03	
N4535	20.30	31.13	0.14	21.59	30.95	-0.04	
N4536	20.29	31.02	0.15	21.50	30.92	0.05	
N4603	20.48	32.57	-0.04	21.61	32.55	-0.06	
N5457	20.33	29.24	0.11	21.31	29.37	0.24	
N7331	20.40	30.78	-0.06	21.52	30.87	0.03	
			$\sigma=0.09$				$\sigma=0.07$

Table III: The effect of Type dependence in the Ursa Major cluster

Galaxy	Type	Log Vflat	m-M B Type	m-M B Single	m-M I Type	m-M I Single
NGC 3726	SBcI-II	2.210	31.02	30.65	30.96	30.82
NGC 3893	SBcI.2	2.274	31.62	31.31	31.53	31.41
NGC 3953	SBbcI	2.348	31.39	31.13	31.37	31.25
NGC 3992	SBbcI	2.384	31.68	31.46	31.58	31.47
NGC 4051	SBbc II _{SY}	2.201	31.20	30.83	30.86	30.72
NGC 4100	SbcI-II	2.215	31.46	31.10	31.27	31.13
NGC 3769	SBbII-III	2.086	31.01	31.16	31.19	31.28
NGC 3949	SbcIII-IV	2.215	31.16	31.38	31.42	31.54
NGC 3972	SBbcIII-IV	2.127	31.53	31.70	31.71	31.81
NGC 4102	SBbII	2.250	31.68	31.92	31.43	31.56
NGC 4217	SbIII	2.250	31.38	31.62	31.04	31.17
NGC 4389	SBbcIV	2.041	31.21	31.34	30.85	30.92
NGC 3729	SBaIII-IV	2.179	31.60	31.80	31.44	31.55
NGC 4138	SO-a	2.167	31.78	31.97	31.12	31.23
NGC 4088	SBcII-III	2.238	30.43	30.66	30.72	30.85
NGC 4085	SBcIII-IV	2.127	31.59	31.76	31.54	31.64
NGC 3917	ScIII-IV	2.130	30.79	31.05	31.09	31.19
UGC 6983	SBcIII	2.029	31.96	32.09	31.96	32.04
Mean All			31.36	31.38	31.27	31.31
Mean Sb/Sc			31.34	31.53	31.29	31.40
Mean ScI			31.40	31.08	31.26	31.13

Table IV: Virgo cluster Hubble Constant

Type	Sample size	Mpc	Vvir	H ₀
Elliptical	27	17.1	1062	62.1
>20 kpc	9	16.8	784	46.7
<20 kpc	18	17.2	1201	69.8
SO-a to Sbc	21	18.4	1010	54.9
Log V > 2.200	10	17.9	865	48.3
Log V < 2.200	11	18.8	1142	60.7
ScII-III to ScIV	18	18.2	1310	72.0
Sbc and Sc I/I-II, seyferts	11	19.4	1854	95.6
All	77	18.0	1226	68.1

Table V: Peculiar motions of Virgo Cluster galaxies larger than 20 kpc

Galaxy	Type	Mpc	Vvir	PV ₇₂
NGC 4254	ScI.3	17.0	2505	+1281
NGC 4303	SBbcI	16.1	1624	+465
NGC 4321	SBbcI	15.2	1682	+588
NGC 4501	SbI-II Seyfert	19.9	2380	+947
NGC 4535	SBcI-II	15.8	1846	+891
NGC 4536	SBbcI-II	14.9	1607	+773
NGC 4527	SbcII	14.1	1776	+761
NGC 4192	SBbII	15.1	-46	-1133
NGC 4216	SBbII	15.3	281	-821
NGC 4548	SBbI-II	16.2	587	-579
NGC 4569	SBabI-II	12.8	-137	-1059
NGC 4365	E/SO	19.9	1299	-134
NGC 4374	E/SO	17.9	1004	-285
NGC 4406	E/SO	16.7	-198	-1400
NGC 4472	E/SO	15.9	940	-204
NGC 4486	E/SO	15.6	1363	+240
NGC 4526	E/SO	16.4	518	-663
NGC 4552	E/SO	14.9	380	-693
NGC 4621	E/SO	17.8	520	-762

Table VI: ScI sample

Galaxy	incl	logVrot	Mpc B	Mpc I	Vcmb
412-10	44	2.362	73.1	78.3	5790
476-15	58	2.146	18.5	18.5	1368
545-21	58	2.299	52.0	57.8	4722
299-4	59	2.267	55.5	57.8	5191
547-14	33	2.265	17.3	17.1	1577
202-26	54	2.134	51.3	44.1	5084
IC 387	46	2.386	73.5	82.8	4480
553-3	50	2.185	56.8	51.8	4507
N3029	48	2.207	71.8	73.1	6911
217-12	42	2.134	41.3	39.8	3693
323-27	60	2.316	52.8	54.5	4140
323-25	59	2.316	50.6	56.5	4518
514-10	39	2.201	32.1	30.8	3034
186-21	65	2.301	66.4	75.9	5539
74-6	61	2.344	30.8	34.3	3049
286-79	58	2.468	46.6	64.9	4751
342-43	63	2.238	51.7	49.7	4839
342-50	56	2.152	35.0	29.5	2426
404-12	35	2.260	48.1	43.1	2393
404-27	67	2.149	37.8	38.0	2278
404-31	65	2.076	50.8	51.1	4156
147-5	34	2.274	85.1	81.7	10678
534-32	69	2.292	89.5	95.1	8894
349-32	58	2.474	79.8	82.8	6534
411-10	41	2.152	79.4	67.3	5574
79-8	52	2.389	113.2	128.2	10500
541-1	59	2.324	71.5	68.9	6067
244-21	46	2.360	105.7	97.3	6983
244-43	60	2.212	67.6	68.6	6025
354-17	73	2.243	50.8	66.7	5440
52-20	63	2.196	63.1	70.8	8068
478-6	54	2.346	76.2	66.1	5103
547-31	49	2.230	17.8	14.9	1421
566-9	53	2.236	49.4	53.7	4481
N3145	62	2.412	44.5	51.1	3998
N4030	40	2.373	33.7	26.2	1814
N5172	58	2.410	52.5	59.2	4306
IC 900	48	2.356	80.2	90.0	7353
445-58	59	2.283	56.5	60.2	5309
186-27	71	2.301	35.0	35.2	2579
107-36	57	2.344	31.3	34.4	3003
237-2	66	2.362	54.5	58.9	4983
N753	46	2.317	51.1	47.2	4644
N4574	51	2.129	38.2	35.6	3250
383-2	64	2.262	64.1	70.8	6453
N3726	53	2.193	15.4	14.7	1072

N3953	62	2.331	18.2	17.8	1240
N4100	77	2.264	21.9	21.1	1273
33-32	56	2.253	50.6	55.2	4785
564-35	49	2.057	10.2	8.6	1188
N3672	69	2.312	29.5	28.2	2221
479-40	66	2.431	108.2	131.8	10338
186-47	69	2.210	60.6	61.4	4482
569-22	50	2.330	50.6	54.2	4091
352-33	42	2.230	73.8	68.2	5441
151-40	47	2.326	91.6	88.7	7277
114-21	52	2.241	94.2	68.2	6284
30-14	31	2.228	66.7	61.9	8207
545-13	34	2.350	86.7	91.6	9907
84-9	59	2.117	55.2	66.7	5054
N2980	62	2.387	68.6	78.3	6050
566-26	47	2.288	42.3	47.6	4099
N4246	62	2.267	55.2	46.8	4064
268-37	53	2.267	68.9	74.1	5175
445-27	60	2.389	88.3	121.9	11735
235-20	51	2.188	42.5	41.9	4515
108-13	64	2.127	39.9	34.5	2823
N268	48	2.582	113.8	171.4	5165
304-16	70	2.312	69.2	74.5	5189
159-2	51	2.233	61.9	60.8	4318
438-15	65	2.215	35.7	42.7	3689
N4541	68	2.396	75.9	91.6	7223
576-51	51	2.223	50.1	48.5	5501
446-58	60	2.360	62.2	61.7	4581
102-22	61	2.461	46.8	58.6	4336
234-22	59	2.314	56.0	59.7	5593
236-37	55	2.248	53.7	70.8	5384
467-27	64	2.288	61.1	53.7	4993
603-22	56	2.380	47.0	46.8	2785
U4308	49	2.182	58.6	38.0	3787
N4835	76	2.252	26.7	22.1	2439
N5161	73	2.227	20.7	23.0	2660
N7610	53	2.172	48.3	53.0	3196

Table VII: Pairs and Groups with intrinsic redshifts

Galaxy	Type	RA	Dec	logVrot	Incl.	m-M(B)	m-M(I)
52-20	SBbcI-II	2 05 44	-71 06 56	2.196	63	34.00	34.25
53-2	Sc	2 13 12	-70 54 49	2.170	90	34.01	34.61
30-14	ScI-II	2 17 57	-76 04 50	2.228	31	34.12	33.96
545-13	ScI	2 24 40	-19 08 28	2.35	34	34.69	34.81
545-18	Sbc	2 27 05	-19 05 40	2.276	76	34.81	35.15
549-30	Sbc	3 53 54	-17 35 36	2.292	70	34.08	34.79
549-31	Sbc	3 54 25	-19 11 26	2.258	68	34.16	34.41
549-37	SBbc	3 56 19	-21 49 15	2.201	51	34.20	34.74
549-40	Sc	3 57 10	-18 46 42	2.442	68	34.61	34.79
550-18	Sbc	4 17 12	-17 51 23	2.373	65	34.16	34.82
550-26	Sbc	4 21 37	-17 55 46	2.230	84	34.13	34.57
31-15	SBbc	3 30 47	-73 46 59	2.318	71	34.69	34.94
31-18	ScII	3 37 43	-72 23 29	2.279	63	34.64	35.19
71-5	SBbcII	18 16 25	-71 34 49	2.371	46	32.85	33.25
71-14	SbcII-III	18 31 07	-71 41 33	2.328	53	32.69	33.21
234-13	SbcII-III	20 22 32	-50 45 11	2.225	67	33.77	34.10
234-22	SbcI-II	20 24 22	-50 25 58	2.314	59	33.74	33.88
234-24	SbcII	20 25 27	-51 31 54	2.265	90	33.86	34.40
234-32	SBbc	20 28 06	-51 41 27	2.233	62	33.90	34.18
186-47	SbcI-II	20 27 46	-52 23 04	2.210	69	33.91	33.94
243-1	Sbc	00 46 07	-42 31 55	2.090	46	34.40	34.49
295-12	ScI	00 50 21	-41 14 34	2.294	55	34.63	34.62
243-3	Sc	00 50 34	-43 03 53	2.029	50	34.39	34.45
243-8	Sb	00 53 46	-45 11 08	2.215	90	34.05	34.21
243-14	ScII	00 56 59	-45 24 41	2.220	67	34.29	34.59
243-20	Sc	01 03 14	-43 00 36	2.037	77	33.92	34.34
243-25	Sbc	01 05 17	-42 54 50	2.097	56	33.99	34.22
243-30	ScII	01 07 10	-42 23 23	2.155	57	34.54	34.52
147-2	Sc	22 35 40	-61 32 51	2.246	68	34.76	35.02
147-5	SBcI-II	22 41 37	-57 36 18	2.274	34	34.65	34.56
147-10	Sbc	22 48 57	-57 53 37	2.281	90	34.75	35.54

Table VIII Excess redshifts of small groups

Group	Vcmb	Mpc B	PV ₇₂ B	Mpc I	PV ₇₂ I	m-M _{72-B}	m-M _{72-I}
30-14	8075	64.3	+3445	71.5	+2927	1.21	.98
545-13	9847	89.1	+3432	99.1	+2712	.93	.70
549-40	8166	69.8	+3140	86.7	+1924	1.05	.58
31-15	8278	85.9	+2093	103.3	+ 840	.63	.23
71-5	3709	35.8	+1131	44.3	+519	.80	.33
234-22	5240	58.6	+1021	66.1	+481	.47	.21
295-12	7360	71.8	+2191	78.0	+1745	.77	.59
147-10	11075	87.9	+4746	101.9	+3738	1.21	.89

Table IX: Serpens Cluster

Galaxy	Type	RA	Dec	logVrot	Incl.	m-M(B)	Vcmb
55198	Sab	15.480	25.748	2.342	75	35.80	10365
55618	SBb	15.618	25.565	2.459	55	36.16	10562
55724	SBbc	15.662	25.742	2.487	63	35.91	15065
55810	Sc	15.695	23.204	2.388	46	36.43	10477
55828	Sa	15.705	23.808	2.362	50	36.12	6989
55979	Sc	15.762	22.879	2.371	32	36.31	12378
56038	Sc	15.789	21.531	2.349	53	35.95	12651
56175	Sbc	15.844	20.382	2.305	55	36.23	11151
56227	Sa	15.858	24.435	2.239	67	35.87	9698
56169	Sc	15.841	18.139	2.507	36	36.06	14095
55721	SBab	15.659	23.199	2.081	56	35.95	11620
55708	Sab	15.655	24.455	2.438	71	35.85	10429
55380	Sa	15.550	25.569	2.221	54	35.78	10177
55872	Sc	15.725	17.313	2.284	50	35.59	9127
56532	Sc	15.974	18.039	2.390	63	35.74	12746
55530	Sc	15.594	21.503	2.200	56	35.65	12697
86655	Sc	15.566	21.790	2.156	68	36.46	7175
56186	Sc	15.847	22.239	2.234	56	35.72	9533
56163	SBa	15.835	25.055	2.301	38	35.69	9609
55213	SBbc	15.484	25.458	2.371	51	35.51	10163

Table X: Serpens Cluster Hubble Constant

Type	Sa/Sab/Sb	Sbc/Sc
Sample size	8	12
Mean distance modulus	35.90	35.96
Mean distance (Mpc)	151.4	155.6
Mean V3k	9931	11438
H ₀	65.6	73.5

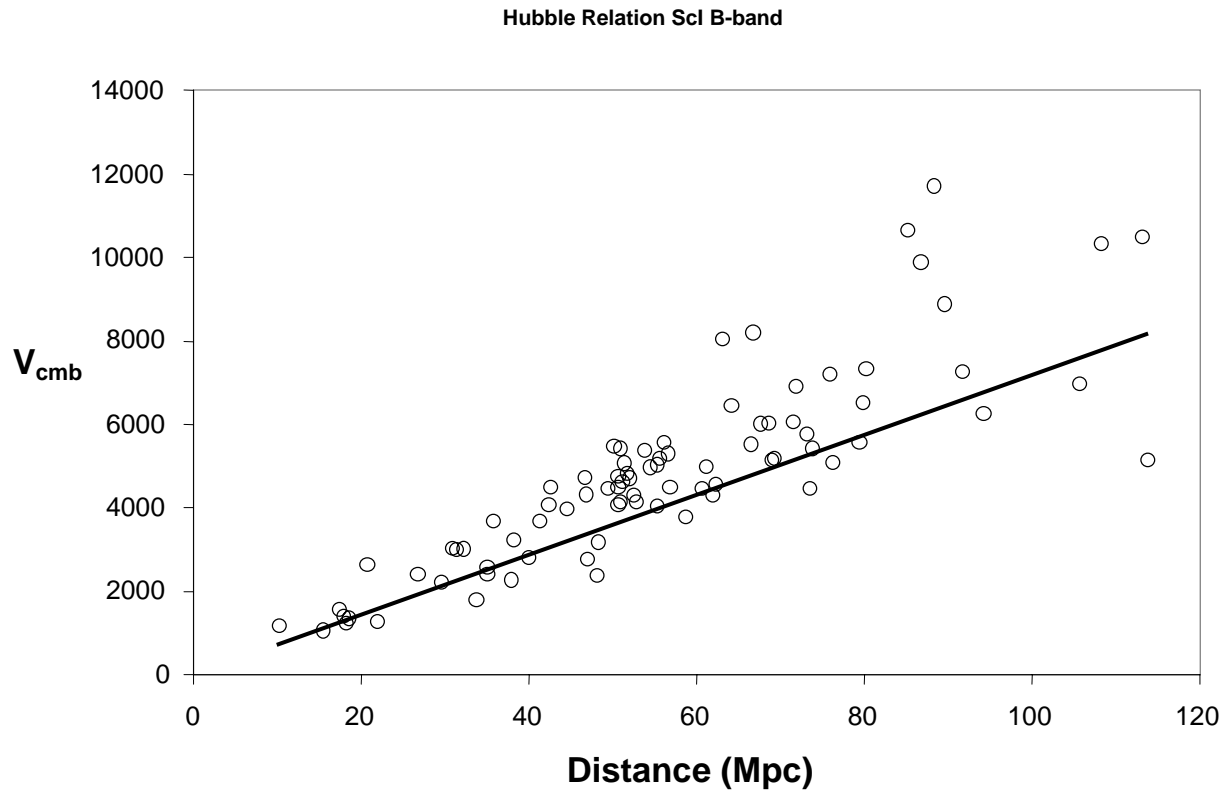


Figure 2: Hubble Relation for ScI galaxies with B-band TF relation. Solid line is a Hubble constant of $72 \text{ km s}^{-1} \text{ Mpc}^{-1}$.

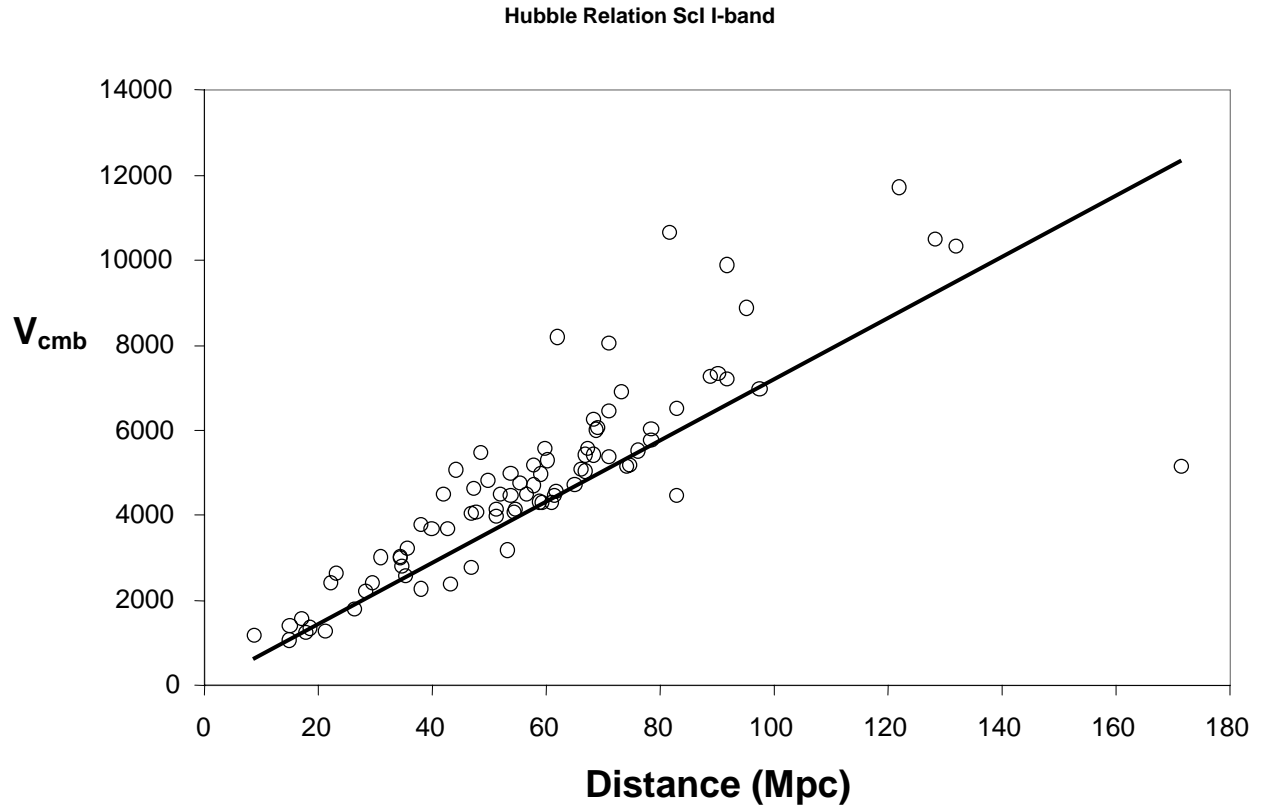


Figure 3: Hubble Relation for ScI galaxies with I-band TF relation. Solid line is a Hubble constant of $72 \text{ km s}^{-1} \text{ Mpc}^{-1}$.

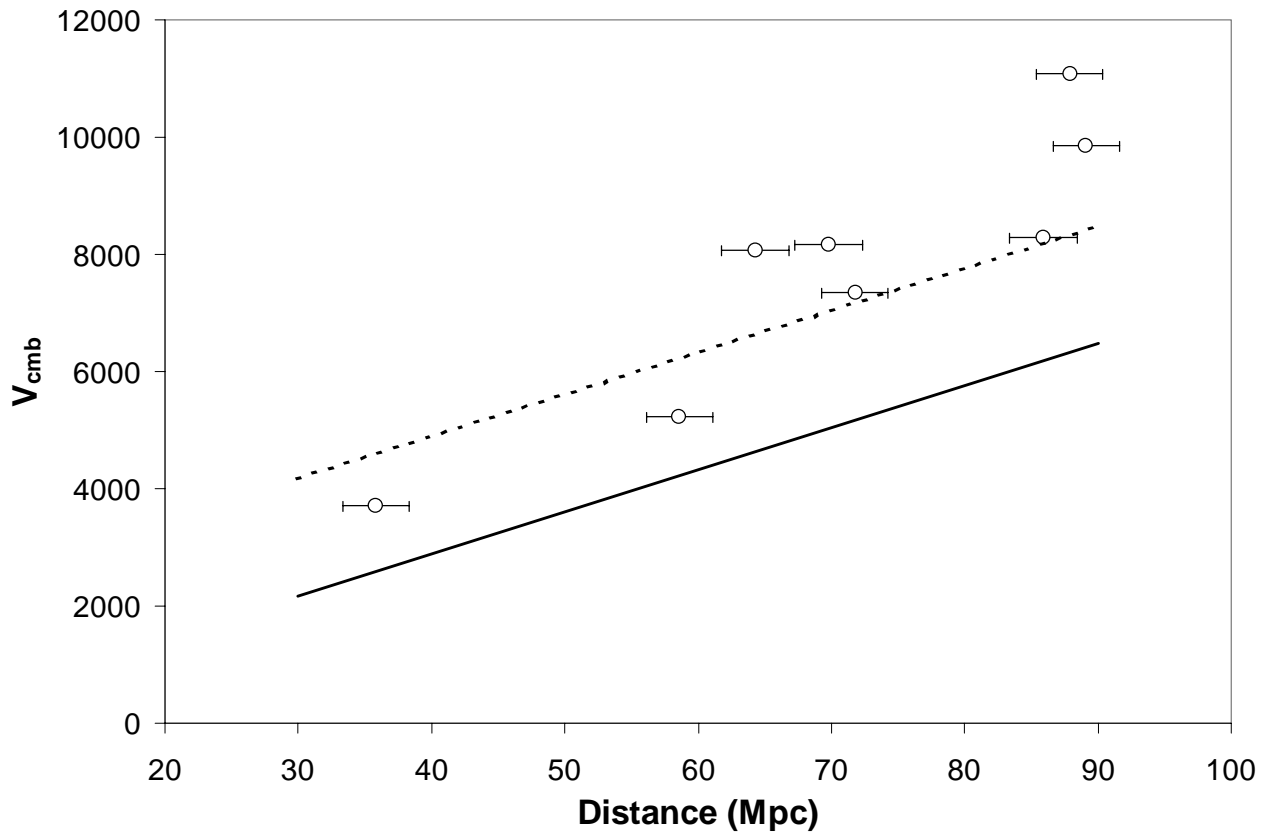


Figure 4 – Hubble Relation for pairs and groups of late type spirals in Table V. Solid line is a Hubble Constant of $72 \text{ km s}^{-1} \text{ Mpc}^{-1}$. Dashed line is a peculiar velocity of $+2000 \text{ km s}^{-1}$. Error bars are $\pm 2.5 \text{ Mpc}$ which is typical distance error individual galaxies in the groups have from the mean group distance.

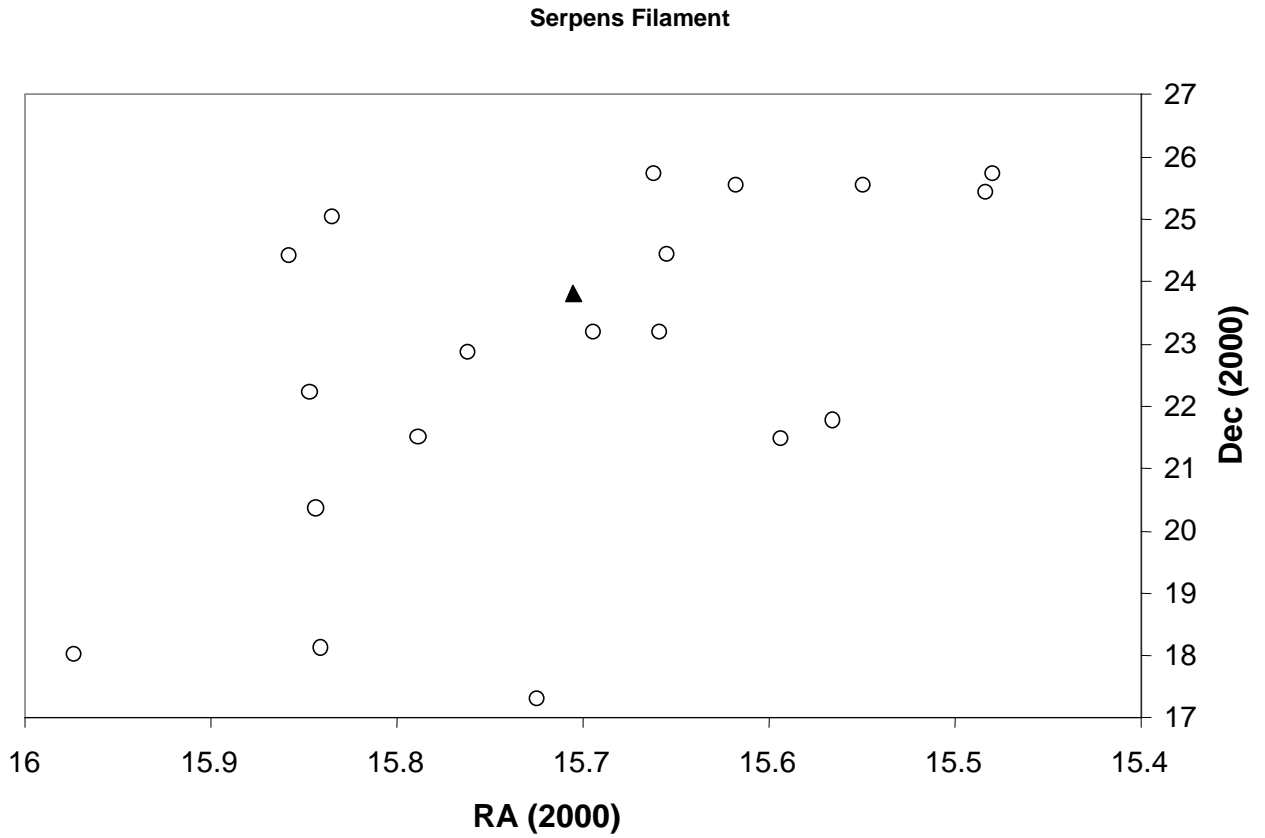


Figure 5 – Galaxies with Tully-Fisher distances which place them in the Serpens filament. The mean distance for the cluster is 154.2 Mpc. Filled triangle is the Sa galaxy PGC 55828 which has a redshift of 6989 km s^{-1} .

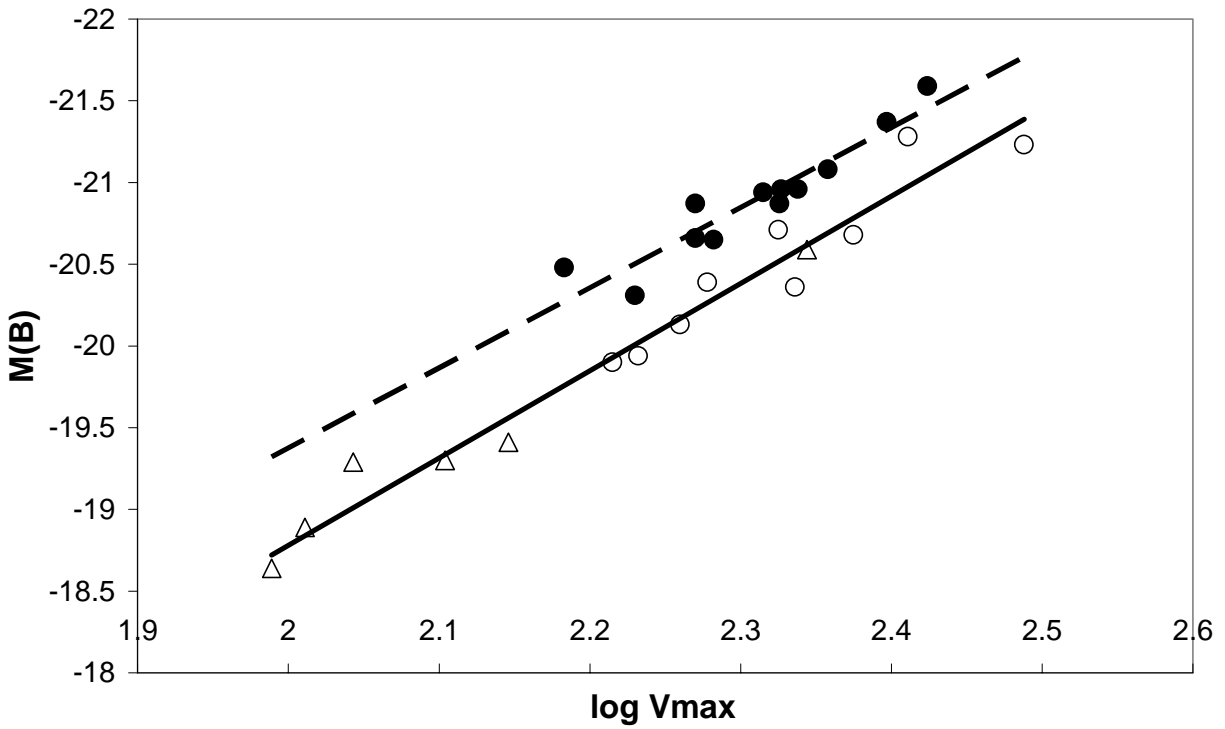


Figure 1 - B-band TF relation for TF calibrator sample. Filled circles are ScI group galaxies. Open triangles are ScIII group galaxies. Open circles are Sb group galaxies. Solid line is least squares fit to the Sb group. Dashed line is least squares fit to ScI group. Note that the ScI group galaxies are systematically more luminous at a given rotational velocity than Sb and ScIII group galaxies.